

CHAPTER 5 - CYCLIC LOAD TESTS ON PILES

5.1. Introduction

The main objective of this experimental program is to investigate the ability of three pile types to withstand cyclic lateral displacements induced by temperature variations. The pile types that are subjected to lateral loading in the laboratory are an H-pile, a pipe pile, and a prestressed reinforced concrete pile. The data from these tests is useful for selecting the type of pile that is best suited for support of integral bridges.

As the superstructure moves back and forth, the foundation piles of an integral abutment bridge are subjected to repeated cyclic loading. Maximum pile stresses take place near the pile cap. Experiments are conducted on a static equivalent of the pile/pile cap system to create maximum stresses near the pile cap. The equivalent system has upside down geometry of the pile/pile cap system under an integral bridge as illustrated in Figure 5.1. The orientation of the pile under an integral bridge is shown on the left-hand side of the figure. The equivalent pile/pile cap system is shown on the right hand side of the figure.

5.2. Design and Construction

Standard plans of integral abutment bridges of the Virginia Department of Transportation (VDOT) were used to design the pile/pile cap samples. The Staunton office of VDOT provided the information necessary for design, and reviewed the plans before advancing to construction.

Construction of the pile specimens was done in the structures laboratory of Virginia Tech. All three piles (H-pile, pipe pile, and prestressed concrete pile) were supplied by VDOT. Construction plans of the pile/pile cap connection for all pile types can be found in Appendix C.

Reinforcements for the pile caps were prefabricated by Resco Steel of Salem, VA. The concrete for the pile caps was provided by New River Concrete of Blacksburg, VA. The formwork and other tasks for the construction were conducted by the technicians at the structures laboratory of Virginia Tech.

Pile lengths and the pile cap dimensions were selected to take full advantage of the available reaction floor in the lab. Piles were 20 feet long when delivered. They had to be cut into proper length. For practical reasons, cap dimensions were kept the same for all piles. Appendix C provides all dimensions of the specimens.

The H-pile was cast into its cap on June 6, 2000. Construction of the pipe pile and the prestressed concrete pile were completed on June 16, 2000 and June 19, 2000, respectively. Concrete slump from each batch was checked before placing the concrete. The slump varied from 4 in. to 4¾ inches. Samples from each batch were taken to ensure proper strength on the test day.

Temporary steel frames were built around the pile/pile caps to prevent piles from moving during concrete placement. The frames also provided additional safety measures against potential danger from other activities in the laboratory.

5.3. Material Properties

5.3.1. Piles

An H-pile, a pipe pile and a prestressed reinforced concrete pile were used in the experiments. The H-pile is a HP10x42, manufactured by Nucor-Yamato Steel of Houston, TX. The heat ID and the grade are 128775 and A572-50 S50, respectively. The pipe pile is made of ASTM A252 Grade 3 steel, and has a 14-inch outer diameter and 0.5 inch wall thickness. The prestressed concrete pile is a 12-inch square standard VDOT pile. This pile has five ½-inch 270 ksi low relaxation steel strands. The prestress on the pile was 920 psi. Table 5.1 summarizes useful properties of the piles. These properties are compiled from material data sheets provided by the manufacturer for each pile.

Table 5.1. Properties of the piles used in the experiments

Pile type	Strength (ksi)*	Area (in ²)	Area moment of Inertia, I (in ⁴)	Young's modulus, E (ksi)
H-pile	54.0	12.4	71.7	29,000
Pipe pile	45.0	21.2	484	29,000
Prestressed reinforced concrete	5.0	144	1,728	4,000**

* 28-day compressive strength for prestressed concrete pile, yield strength for steel piles
 ** Determined by $E = 57,000\sqrt{f'_c}$, where f'_c = compressive strength of concrete (5,000 psi)

5.3.2. Concrete

Pile caps were cast from locally purchased VDOT Class A4 concrete. This type of concrete has a minimum 28-day strength of 4,000 psi, an air content of $6.5 \pm 1.5\%$, and a minimum cement content of 600 lbs per cubic yard of concrete. Coarse, non-polishing aggregate is used.

Because of the time constraints, early strength accelerators were added to concrete mixes of the caps for the pipe pile and the prestressed concrete pile. This additive produces the 28-day strength in about 7 days.

Concrete samples from each pile cap were collected and compressive strengths of these samples were determined on the day of testing. Compressive strength and other useful properties of concrete for each pile cap are summarized in Table 5.2. Young's modulus of the concrete is calculated by $E = 57,000\sqrt{f'_c}$, where f'_c is the strength on the test day in psi.

Table 5.2. Strength properties of concrete of pile caps

Pile type	Age on test day (day)	Strength on test day (psi)	Slump (in.)	Young's modulus, E (ksi)
H-pile	18	4,200	4	3,700
Pipe pile	11	4,500	4 ³ / ₄	3,800
Prestressed concrete	11	4,500	4 ³ / ₄	3,800

5.4. Load Test Setup

The setup of the load tests consists of three major tasks:

1. Mounting the pile cap onto the reaction floor,
2. Application of the vertical load to the pile, and
3. Application of the lateral load to the pile.

5.4.1. Mounting pile caps on reaction floor

Six threaded rods are placed in each pile cap during construction such that the rods extend out of the cap. On each side of a pile cap, an 8-foot segment of a HP10x42 is

bolted on the threaded rods that are protruding from the pile cap. Figure 5.2 shows the locations of the threaded rods, and the floor-mounting plan of the pile caps. The HP10x42 segments are bolted down to the reaction floor at each corner by specially made L-shaped steel elements as pictured in Figure 5.3. A total of four of these elements are used for each pile cap.

Torsional capacity of HP10x42 segments was improved before testing the prestressed concrete pile by using stiffeners between the two flanges of the HP10x42 segments. Four 1-inch thick plates were used as stiffeners for each HP10x42 segment.

5.4.2. Application of vertical load

The application of the vertical load was achieved through a specially designed system. The system consists of three components:

1. A steel beam,
2. Two hydraulic rams, and
3. Two support elements called gravity load simulators (GLS).

These components can be seen in Figure 5.4.

The steel beam is first bolted on the top of the pile to be tested. Then the rams are hung by pins from each corner of the beams. The other ends of the rams are connected to the middle pin of the GLSs as seen in Figure 5.4. A GLS is a simple frame that has five pinned connections. These pins are located on each corner of the GLS. A view of a GLS is pictured in Figure 5.5.

The unique structure of the gravity load simulators and the pinned connections of the hydraulic rams keep the rams vertical for any given lateral displacement of the pile being tested. A tension load cell was also placed between each ram and each GLS.

Both of the rams are controlled by a single pump to ensure even distribution of the vertical load on each side of the top beam. Each ram provides half the vertical load acting on the pile.

5.4.3. Application of lateral load

A computer controlled MTS hydraulic actuator capable of applying ± 50 kips of load and ± 3 inches of displacement was used to apply cyclic lateral loads. Views of the actuator during testing are shown in Figure 5.6.

The actuator can be used as either load or displacement controlled. Actuator control is provided by a MTS 458.10 MicroConsole unit with a 458.14 AC displacement controller, a 458.12 DC load controller, and a 458.90 function generator. All tests were run displacement controlled.

5.4.4. Instrumentation and data acquisition

Data from measuring devices were collected into a MEGADAC 3108AC unit made by Optim Electronics. The unit converts the analog voltage readings from the measuring devices into digital signals. Digital signals are then sent to a PC, from which signals are read by the TCS data acquisition software.

Three types of measuring devices were used:

1. Displacement
2. Load
3. Strain

Displacement measurements were made by wire pot transducers. Each transducer was calibrated on-site immediately before it was put into service. Five transducers were used during each test. For convenience, the locations of the transducers were kept the same in all tests. Three of these transducers measured the lateral displacements of the pile while the remaining two were used to record the lateral displacement of the pile cap. Table 5.3 shows the locations where the lateral pile displacements were measured.

Figure 5.7 shows a picture of a steel stand placed on the pile cap. This steel stand was placed in the middle of the pile cap. Two transducers measured the displacements of the steel stand at two locations: 4 in. and 13 in. above the pile cap. The data from these two transducers is used to calculate the rotation of the pile cap. A picture of a wire pot transducer is shown in Figure 5.8.

In addition to displacement transducers, the MTS actuator has a built-in LVDT to measure the displacement of the actuator. Readings of this LVDT reflect the combined displacement of the pile at the location where the load is applied and the displacement at the support of the actuator.

Three load cells were used. One of the load cells was built into the MTS actuator. This load cell, capable of measuring both tension and compression loads, was used to measure the lateral load transferred to the pile. The other load cells are tension load cells, which were used to monitor the vertical loads applied to the pile. Calibrations were checked before using these load cells. One of the tension load cells needed to be re-calibrated. It was re-calibrated using a Satek universal testing machine. The load cell exhibited a linear response without any hysteresis.

Table 5.3. Locations of transducers used to measure the lateral deflections of piles

Transducer No.	Distance of measurements from pile cap (in.)
WP-7	7
WP-28	28
WP-53	53

Strain gages were purchased from the Measurements Group and installed according to the manufacturer's instructions. CEA-06-250UN-120 and N2A-06-40CBY-120 gages were used on steel and concrete surfaces, respectively. The steel gages were ¼ in. long while the concrete gages were 4 in. long. Both gages had 120-ohm resistance. The gage factors were 2.065 and 2.100 for the steel and concrete gages, respectively.

Locations of the strain gages are shown in Figure 5.9. The H-pile had 4 gages near the pile cap: two were located at the opposite tips of the flanges, and the other two were used as backup near the tip of the flanges. The pipe pile had 4 gages: two were located near the pile cap, one located 55 in. above the pile cap, and the last one located 70 inches

above the pile cap. The gage located 55 in. above the pile cap was slightly above the concrete cast into the pipe. The prestressed concrete pile had two gages. Both of which were placed near the pile cap on the opposite sides of the pile.

5.5. Test Program

The purpose of the test program is to simulate the effects of lateral loading induced by temperature changes over the expected life of integral bridges, and evaluate damage to pile/pile cap system under working stress conditions. The life span of an integral bridge is deemed to be 75 years.

Approximately 27,000 small cycles are necessary for a 75-year simulation of bridge life. To input this many cycles, one would like to use the highest excitation frequency possible. Before setting the excitation frequency, natural frequencies of each pile were calculated using Equation 5.1 (James et al., 1994).

$$f_n = \frac{1}{2} \sqrt{\frac{g}{W} \left(\frac{EI\pi^2}{32l^3} - \frac{W}{8l} \right)} \quad (5.1.)$$

Where,

f_n = natural frequency of the pile

g = acceleration of the earth,

W = weight of each pile plus any vertical load, and

l = length of each pile (102 inches).

Table 5.4 shows the natural frequency calculated for each pile for a vertical load of 70 kips. For smaller vertical loads, the natural frequency is higher.

As the excitation frequency approaches to the natural frequency in a load-controlled test, displacements become significantly large. These large displacements can result in an unintended failure of the pile because of the resonance phenomenon. If the excitation frequency remains below the 25% of natural frequency, displacements remain very close

to those resulting from static loading (James et al., 1994). Because the experiments are displacement controlled, it is possible to set the excitation frequency higher than the 25% of natural frequency. The final decision of the excitation frequency was made after several trial runs under various vertical loads. It was found that there is some amplification of displacements for frequencies above 0.7 Hz for the H-pile. The operating frequency was set as 0.6 Hz for small cycles for all pile types. For the large cycles, the excitation frequency was selected as 0.1 Hz.

Table 5.4. Estimated natural frequencies of piles for 70 kips of vertical load

Pile type	f_n , Natural frequency (Hz)
Steel HP10x42	0.85
Pipe pile	2.35
Prestressed reinforced concrete	1.54

5.5.1. Steel H-pile

Experiments on the H-pile oriented in weak-axis bending were conducted in order to investigate the damage due to cyclic loading induced by temperature variations. Effects of the temperature variations were modeled as presented in Chapter 3 in the test series HP-BB. In order to demonstrate the importance of this model, two more experiments, HP-AA and HP-CC, were conducted by considering only the seasonal displacement cycles. Test HP-AA was conducted before the test HP-BB while test HP-CC was conducted after the test HP-BB. Finally, in test HP-DD, an attempt was made to fail the H-pile by using the maximum displacement stroke of the MTS actuator. Designation of the experiments and brief description of each are tabulated in Table 5.5.

In test HP-BB, the maximum stress level was targeted as 50% of the nominal yield capacity of the pile. The test was run displacement controlled. Strain gage readings were

collected before testing the pile in order to determine the relationship between the displacement at the top of the pile and the maximum stress in the pile. Subsequently, the displacement of the MTS ram was set to generate the target stress level. The method proposed in Chapter 3 was used with a slight modification to apply the small cycles. For each year of the bridge life, a large displacement cycle and 365 small daily cycles were imposed on the pile. Approximately 1/3 of the maximum displacements is used to simulate daily temperature variations. Small cycles were applied in three groups. Table 5.6 summarizes the representation of a year of temperature variations in the experiments.

Table 5.5. Description of the tests conducted on the steel H-pile

Designation	Description
HP-AA	Application of 75 major cycles on the H-pile. Maximum target stress: ± 17 ksi.
HP-BB	Simulation of 75-year temperature variations by 75 large cycles and 27,375 smaller cycles following test HP-AA. Maximum target stress: ± 17 ksi.
HP-CC	Application of 75 major cycles on H-pile following test HP-BB. Maximum target stress: ± 17 ksi.
HP-DD	Attempting to fail the H-pile by using the maximum displacement stroke of the hydraulic actuator.

Table 5.6. Representation of one year of temperature effects in the laboratory

Cycle designation	Targeted stress range (ksi)	Mean stress level (ksi)	Excitation frequency (Hz)	Number of cycles
HP-L1	-17 to +17	0	0.1	1
HP-S1	-8 to +8	0	0.6	183
HP-S2	0 to +17	8.5	0.6	91
HP-S3	-17 to 0	-8.5	0.6	91

5.5.2. Steel Pipe Piles

Due to last minute changes made in the size and detail of the pipe pile by the project sponsor, the pipe pile could not be tested in the same manner as the other piles. The test system was capable of imposing stresses of up to 6 ksi in the pipe pile. About 2300 cycles at 0.1 Hz. were imposed.

5.5.3. Prestressed Reinforced Concrete Pile

Experiments on the prestressed reinforced concrete pile were conducted in order to investigate the damage due to cyclic loading induced by temperature variations. Effects of the temperature variations were modeled similar to the H-pile test. Three series of experiments were conducted. These are, in the order conducted, CP-AA, CP-BB, and CP-CC. Designation of the experiments and brief description of each are tabulated in Table 5.7. In test CP-AA, 150 displacement cycles were imposed for the maximum initial target stress of 2,500 psi. In test CP-BB, 75 year of bridge life simulated similar to the H-pile test HP-BB by imposing one large cycle and 365 small cycles for each year. Approximately 1/3 of the maximum displacements is used to simulate daily temperature variations. Small cycles were applied in three groups. In test CP-CC, 75 displacement cycles were imposed in the same manner as the test CP-AA. Table 5.8 summarizes the representation of a year of temperature variations in the experiments.

Table 5.7. Description of the tests conducted on the concrete pile

Designation	Description
CP-AA	Application of 150 major cycles on prestressed concrete pile. Maximum target stress: 2.5 ksi.
CP-BB	Simulation of 75-year temperature variations by 75 large cycles and 27,375 smaller cycles following test CP-AA. Maximum target stress: 2.5 ksi.
CP-CC	Application of 75 major cycles on prestressed concrete pile following test CP-BB. Maximum target stress: 2.5 ksi.

Table 5.8. Representation of one year of temperature effects in the laboratory

Cycle designation	Targeted stress range (ksi)	Mean stress level (ksi)	Excitation frequency (Hz.)	Number of cycles
CP-L1	-2.50* to +2.50	0	0.1	1
CP-S1	-1.25* to +1.25	0	0.6	183
CP-S2	-1.25* to 0.00	-0.625*	0.6	91
CP-S3	0.00 to +1.25	+0.625	0.6	91
*Because of tension cracks, concrete does not experience this tension stress.				

5.6. Results

5.6.1. H-pile Tests

Maximum displacement of the pile, measured 53 inches above the pile cap, and the measured strain is summarized in Table 5.9. Data was collected at the beginning of each test series and at selected intervals. In HP-AA and HP-CC series, data was collected during the cycles of 0, 10, 50, and 75. In series HP-BB, 75-years of bridge life was simulated. Each year is simulated by a combination of small cycles and a large cycle as shown in Table 5.6. Data was collected similar to other series for the simulated years of 0, 10, 50, and 75.

Table 5.9. Maximum measured displacement and strain in H-pile

Test series	Maximum displacement (in.)	Bending strain ($\mu\epsilon$)	Vertical load (kips)	Strain imposed by vertical load ($\mu\epsilon$)
HP-AA	0.5	580	38	87
HP-BB	0.5	580	38	87
HP-CC	0.5	580	38	87
HP-DD	0.85	1140	38	87

Figure 5.10 shows the relationship between the displacement and the lateral load for the HP-AA series. The first and the 75th cycle are shown in the figure. Displacement and lateral load data were measured 53 inches and 86 inches above the pile cap, respectively. The figure indicates that 75 cycles do not cause any damage either in the pile or in the pile cap, which was also observed during the experiments. The maximum bending strain on the pile was about 580 $\mu\epsilon$. An additional strain of 87 $\mu\epsilon$ (3 ksi compression stress) was also applied to the pile by the vertical loading rams.

A similar plot obtained from the HP-BB series is shown in Figure 5.11. A comparison between the first (BB-00) and last (BB-75) cycles indicates that there is a slight reduction, about 5%, in the lateral load for a given displacement.

The fact that there is no reduction in the load during HP-AA series and that there is some reduction in the lateral load in the HP-BB series indicates the importance of daily temperature cycles. Series HP-CC was conducted to emphasize this point. Lateral load-displacement behavior in the HP-CC series can be seen in Figure 5.12. As seen in the figure, there is no reduction in the lateral load for a given displacement.

The HP-DD series was a static load test. A maximum of 1140 $\mu\epsilon$ bending strain was applied in addition to the 87 $\mu\epsilon$ strain (3 ksi compression stress) from the vertical load. As seen in Figure 5.13, the pile sustained this load without losing its linear load-displacement response. A strain of about 1200 $\mu\epsilon$ corresponds to the nominal yield stress of 36 ksi. Observations of the pile and the pile cap showed no sign of distress.

For a given load, it was found that the maximum measured strain is about half of the strain calculated for a fixed-end column as shown Figure 5.14. This can be explained by the fact that the pile is actually not 100% fixed at the pile/pile cap interface.

Pile displacements were measured along the pile and shown in Figure 5.15 for selected lateral loads. The figure indicates that the slope at the bottom of the pile is not zero, which indicates that the pile behaves as a partially fixed column.

5.6.2. Pipe Pile Tests

The stiffness of the pipe pile was almost twice the stiffness of its cap. Coupled with this and the limited rotational capacity of the steel elements used for mounting the cap

onto the reaction floor caused the pile cap to rotate more than that of the H-pile tests. When the pile cap rotates, stresses build-up around the edges of the pile cap. These higher stresses caused the concrete in this region to chip off during initial trials. Figure 5.16 shows two pictures of minor damage in pile caps. The top picture shows the debris of the cracked concrete after the cap was removed. It illustrates where the damage was concentrated. The lower picture shows a side view of the pile cap after the test was completed.

A constant vertical load could not be maintained on the pile. The stresses from the vertical load would have been 2 ksi, which is not significant. Therefore, it was decided to omit the application of the vertical load. Approximately 2,300 cyclic lateral loads were applied to the pile at a distance 86 inches above the pile cap. These cycles generated a maximum bending stress of about 4 ksi in the pile. Figure 5.17 shows the lateral load-displacement response of the pile for the first and the 2,300th cycle. Lateral displacement and lateral loads were measured 53 in. and 86 in. above the pile cap, respectively.

Pile displacements and strains were measured along the pile and shown in Figure 5.18 and 5.19, respectively, for selected lateral loads. The strain distribution in Figure 5.19 has a bilinear shape. This is because of the fact that the pipe pile is filled with reinforced concrete up to about 50 inches from the pile cap. This reinforced concrete inside the pile increases the moment of inertia of the pile and thereby reduces the bending strains.

5.6.3. Prestressed concrete pile tests

Data was collected at the beginning of each test series and at selected intervals. In CP-AA and CP-CC series, data was collected during the cycles of 0, 10, 50, 75, and 150. In series CP-BB, 75-years of bridge life was simulated. Each year is simulated by a combination of small cycles and a large cycle as shown in Table 5.8. Data was collected similar to other series for the years of 0, 10, 50, and 75.

Tension stresses are initially carried by the concrete in a reinforced concrete element. As soon as the tension capacity of the concrete is reached, the concrete cracks. In order to detect the tension capacity of the concrete, data was recorded in the initial trial cycles.

In the first trial cycle, tension cracks at the bottom of the pile have developed. One of the cracks has passed through one of the strain gages, and left it useless. Data obtained from this strain gage until its failure is presented in Figure 5.20. Displacement values in the figure are measured 53 inches above the pile cap. The other strain gage was operable during the testing period. Data from the first cycle of this gage is presented in Figure 5.21. It should be noted that these two strain gages are placed on opposite sides of the pile and that loading in the opposite direction is required to generate tension stresses on these gages. As can be seen in Figures 5.20 and 5.21, the tension capacity of the pile is between 100 and 130 $\mu\epsilon$. These correspond to a stress range of about 400 to 500 psi for $E=4000$ ksi. Pictures of the tension crack in the pile are shown in Figure 5.22.

Table 5.10 summarizes the maximum displacement of the pile, measured 53 inches above the pile cap, and the maximum lateral load measured. No vertical load could be applied to the pile because of equipment limitations. The compression stress from the vertical load would have been less than 500 psi.

Figure 5.23 shows the relationship between the displacement and the lateral load for the CP-AA series. In the figure, the first, 10th, 50th, and 150th cycles are shown. Displacement and lateral load data was measured 53 inches and 86 inches above the pile cap, respectively. For a given displacement, the figure indicates continuous reductions in the bending stresses with increasing cycles.

Table 5.10. Tests conducted on the concrete pile

Test series	Maximum Displacement (in.)	Maximum measured lateral load (kips)
CP-AA	0.7	9
CP-BB	0.8	7
CP-CC	1.0	7

It was observed during testing that tension cracks progressively developed in the pile starting from the bottom of the pile to the top of the pile. The distance between the two

adjacent cracks varied between 7 to 11 inches. A total of five tension cracks were visible. The first one was about 2 inches above the pile cap while the last tension crack was about 40 inches above the pile cap. A picture of the pile was taken during the CP-AA series and is presented in Figure 5.24 to show the locations of the tension cracks.

Tension cracks gradually enlarged as the load cycles continued. Coupled with this observation and the progressive nature of the development of the tension cracks are probably responsible for the continuous reductions in pile stresses.

Lateral load-displacement relationships during CP-BB and CP-CC test series are shown in Figures 5.25 and 5.26, respectively. As seen in the figures, the reduction in lateral load for a given lateral displacement continued to take place in the CP-BB series. This appears to be associated with the progressive deterioration caused by the tension cracks. In CP-CC series, no more reduction in lateral load occurred. It is clear from the load-displacement behavior that the damage in the concrete pile is more pronounced in the early cycles. It also appears that larger cycles create most of the damage.

5.7. Discussion

5.7.1. Steel H-pile

The H-pile bent about its weak axis exhibited the best behavior among the piles tested. The pile sustained stresses in excess of 20 ksi in cyclic loading and 35 ksi in static loading without any sign of distress. This is most likely to be associated with the low flexural stiffness of the H-pile. It may be possible that this pile would survive temperature-induced cyclic loads up to its nominal rated capacity of 36 ksi. Coupled with the tests results and the ease of availability and workability of the H-piles make it the best choice for support of integral bridges.

5.7.2. Pipe pile

A 14-inch steel pipe pile with 0.5-inch wall thickness has a stiffness that is significantly larger than that of the H-pile tested. An abutment supported by this type of

pile would be subject to stresses that are much higher than an H-pile with weak axis orientation would. It seems that the pipe pile would survive the temperature-induced cyclic loading. However, there is some evidence in the test that the abutment would be the first to fail if either one were to fail. This is because of the fact that for a given displacement, stiffer piles attract higher lateral loads.

5.7.3. *Prestressed reinforced concrete pile*

Test results of the concrete pile do not reflect the effect of the vertical load, which would be expected to be detrimental. It is anticipated that the damage in the prestressed concrete pile would have been even more severe if a vertical load had been maintained on the pile. As the pile is pushed laterally, the concrete area available to resist the compression stresses from the vertical load became smaller because of the tension cracks that had developed. At the end of the tests, it was observed that the contact area had dropped below 20% of the original cross-sectional area of the pile. Under this condition, the compressive stress induced by the vertical load would be considerably increased. Therefore, it appears that the use of concrete piles to support integral abutment bridges is not the best choice, because of the possibility that they may crack and suffer cumulative damage under cyclic loading.

5.8. **Conclusions and Recommendations**

Based on the findings of this study, the following conclusions and recommendations are drawn concerning the piles supporting integral bridges.

- It appears that steel H-piles oriented in weak-axis bending are the best pile types for support of integral abutment bridges. Experiments simulated 75 years of bridge life by applying over 27,000 displacement cycles, and indicated no sign of distress for this pile type.

- Pipe piles have significantly higher flexural stiffness than do steel H-piles in weak axis bending, for a given pile width. This creates an undesired condition for the shear stresses in the abutment. For a given displacement, stresses in an abutment supported by pipe piles will be higher than stresses in an abutment supported by steel H-Piles in weak axis bending. In other words, the abutment is in more jeopardy if stiff piles such as pipe piles are used. Therefore, stiff pipe piles are not recommended for support of integral bridges.
- Concrete piles are not recommended for integral bridge support because under lateral loads, tension cracks progressively worsen and significantly reduce the vertical load carrying capacity of these piles.
- Tests indicate that seasonal temperature variations are more important for the concrete pile. The total number of daily temperature cycles appears to be more important for the H-pile.
- It appears that stiff piles increase the likelihood of abutment distress. A choice has to be made by the designer whether the pile or the abutment should fail first if one of the two were to fail. Less stiff piles would serve well if the integrity of the abutment is more important.
- Tests also indicate that piles are not fully fixed at the pile/pile cap interface. In the H-pile and pipe pile tests, measured stresses were about half of the theoretical stresses of the fully fixed-head piles.

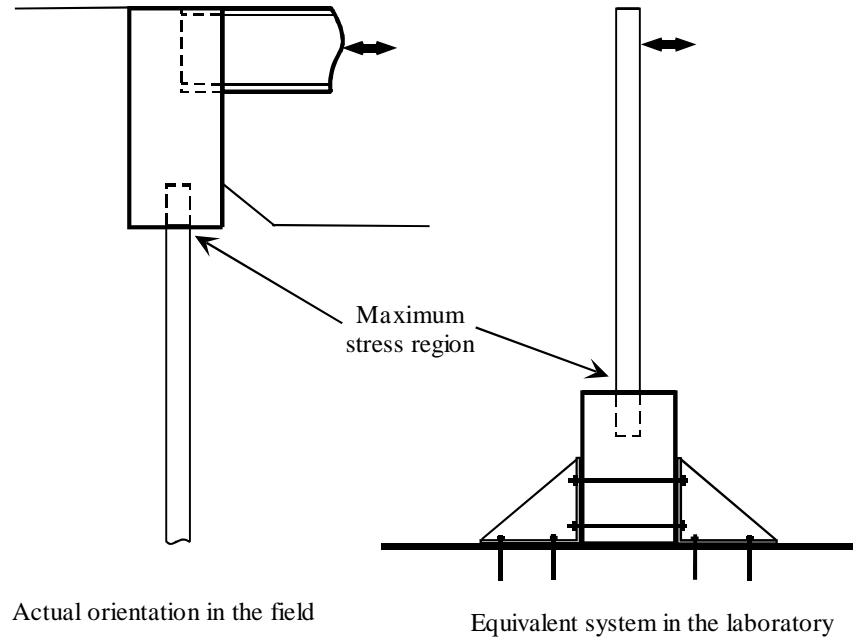


Figure 5.1. Static equivalent of the pile/pile cap system in the laboratory

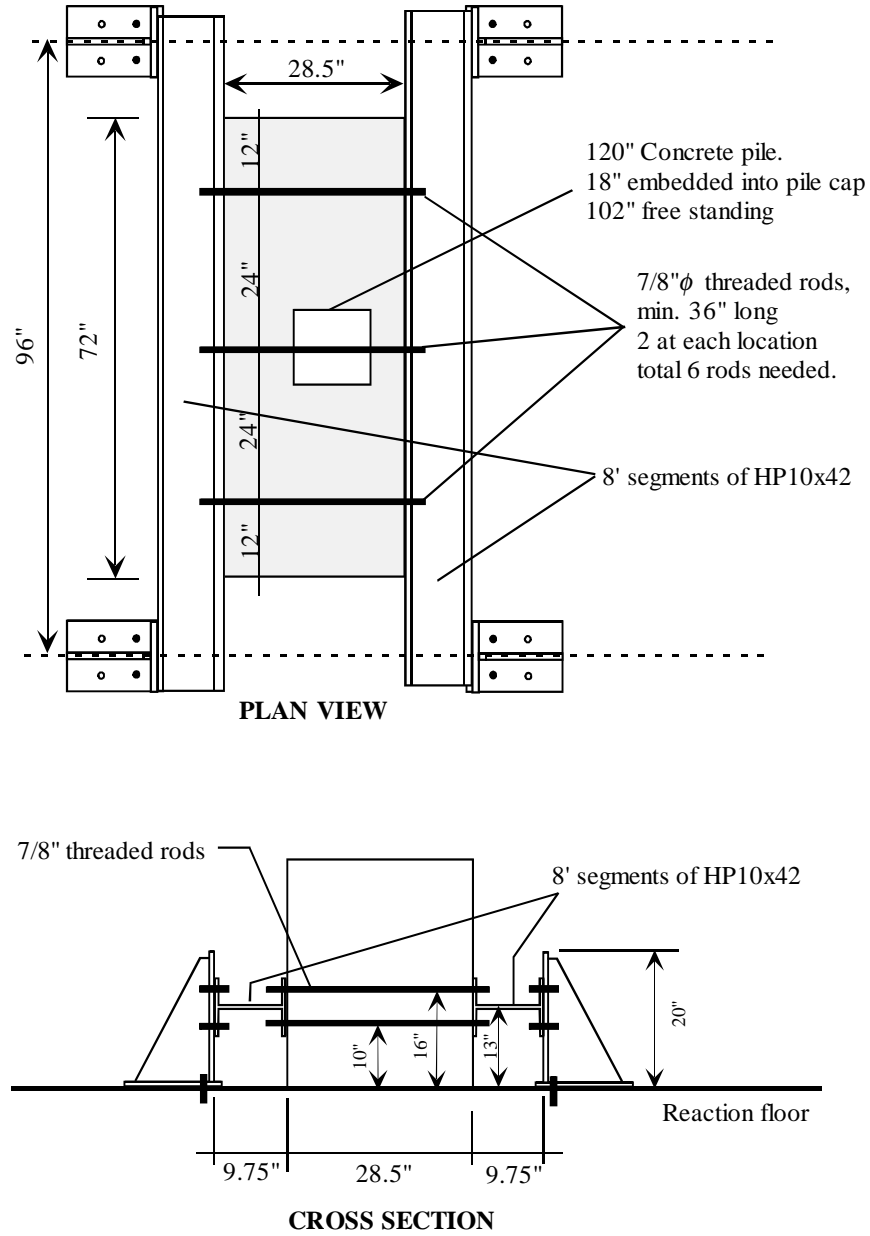


Figure 5.2. Schematic illustration of mounting pile caps on reaction floor



Figure 5.3. Mounting pile caps to reaction floor by L-shaped steel elements



Figure 5.4. Vertical load application to piles



Figure 5.5. Gravity load simulator (GLS)



Figure 5.6. Views of the MTS actuator during cyclic lateral loading



Figure 5.7. Picture of the steel stand used to measure rotation of the pile cap



Figure 5.8. Picture of a typical wire pot transducer used to measure displacements

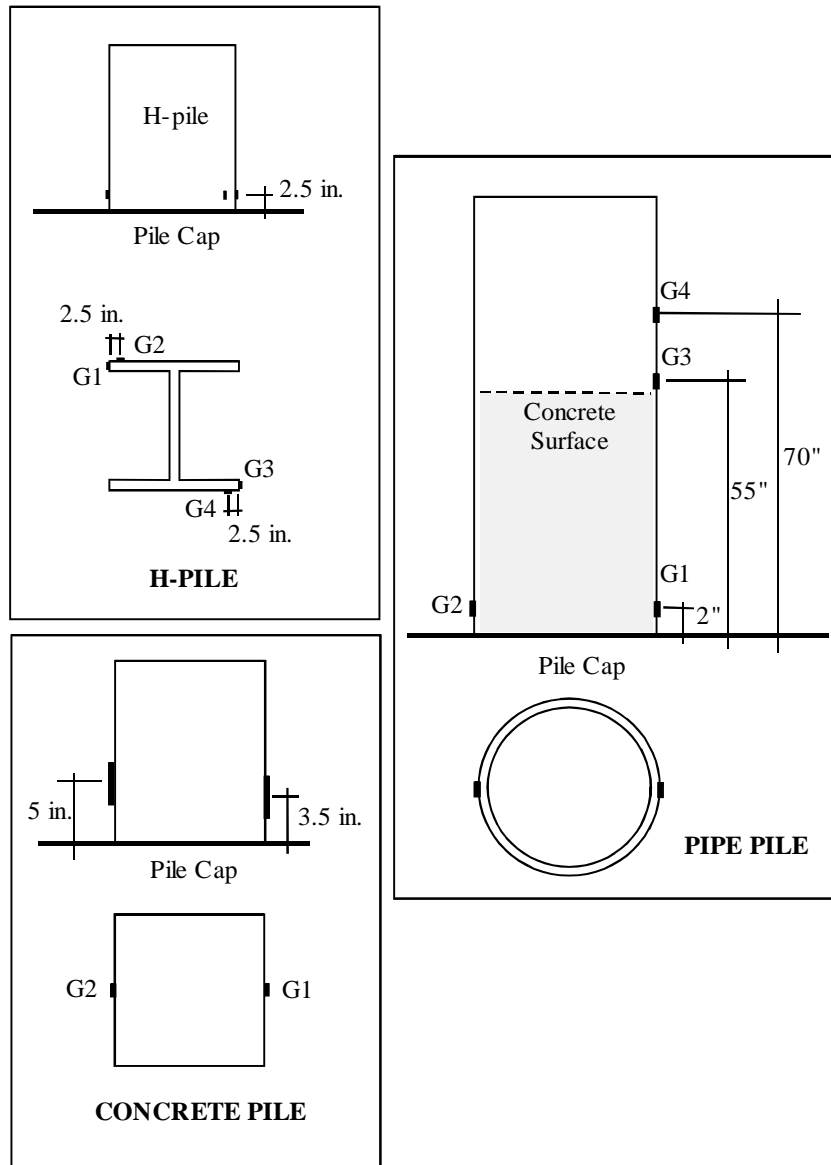


Figure 5.9. Locations of strain gages used in the experiments

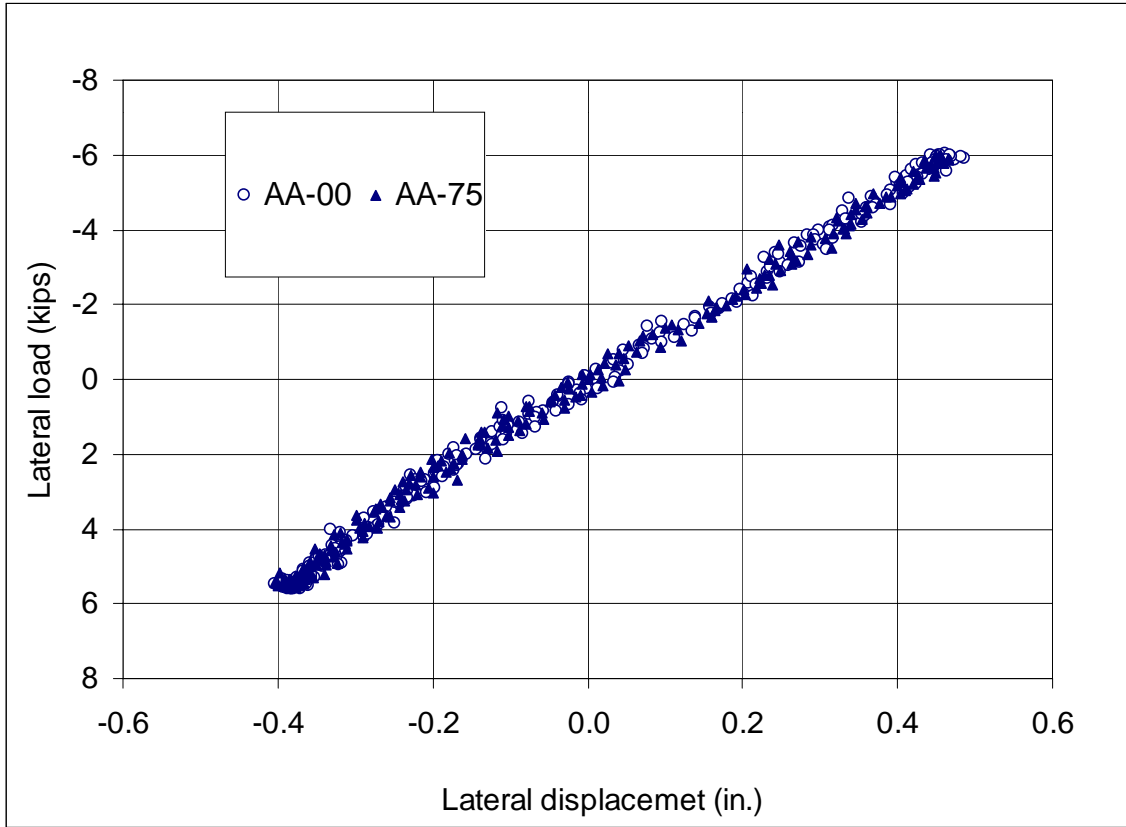


Figure 5.10. Lateral load vs. displacement relationship in HP-AA series

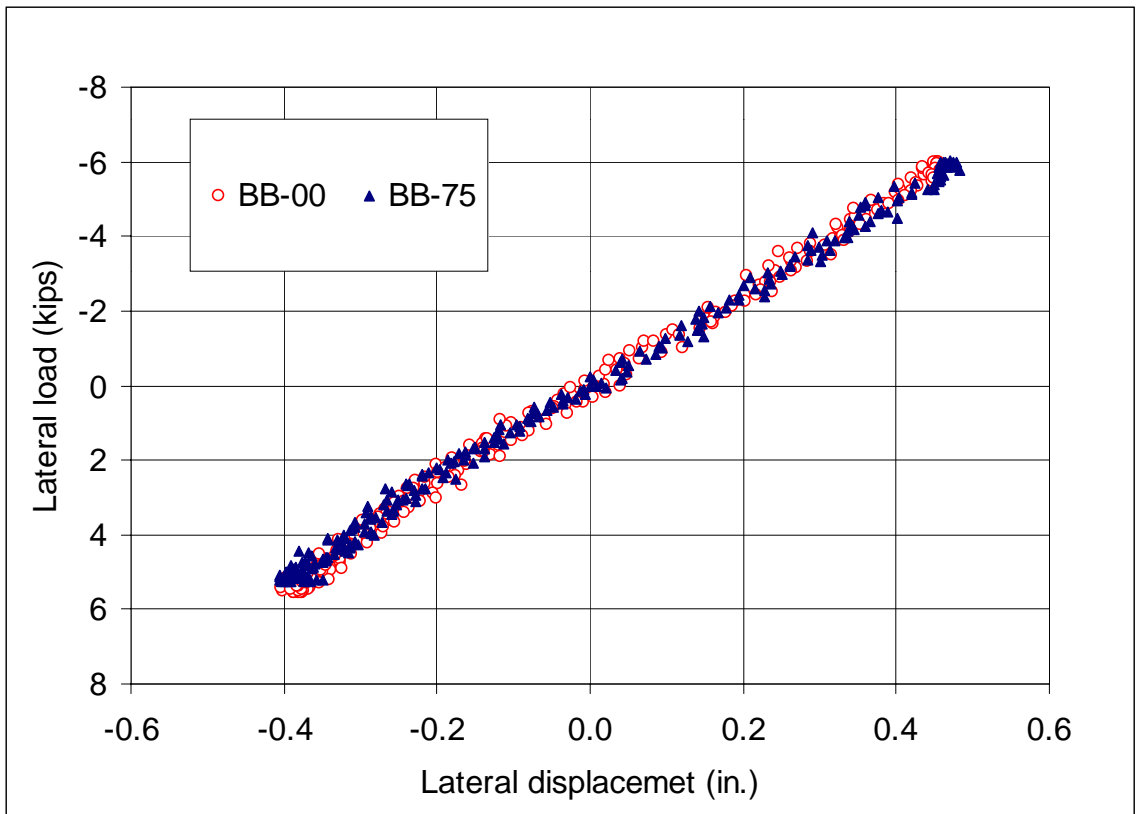


Figure 5.11. Lateral load vs. displacement relationship in HP-BB series

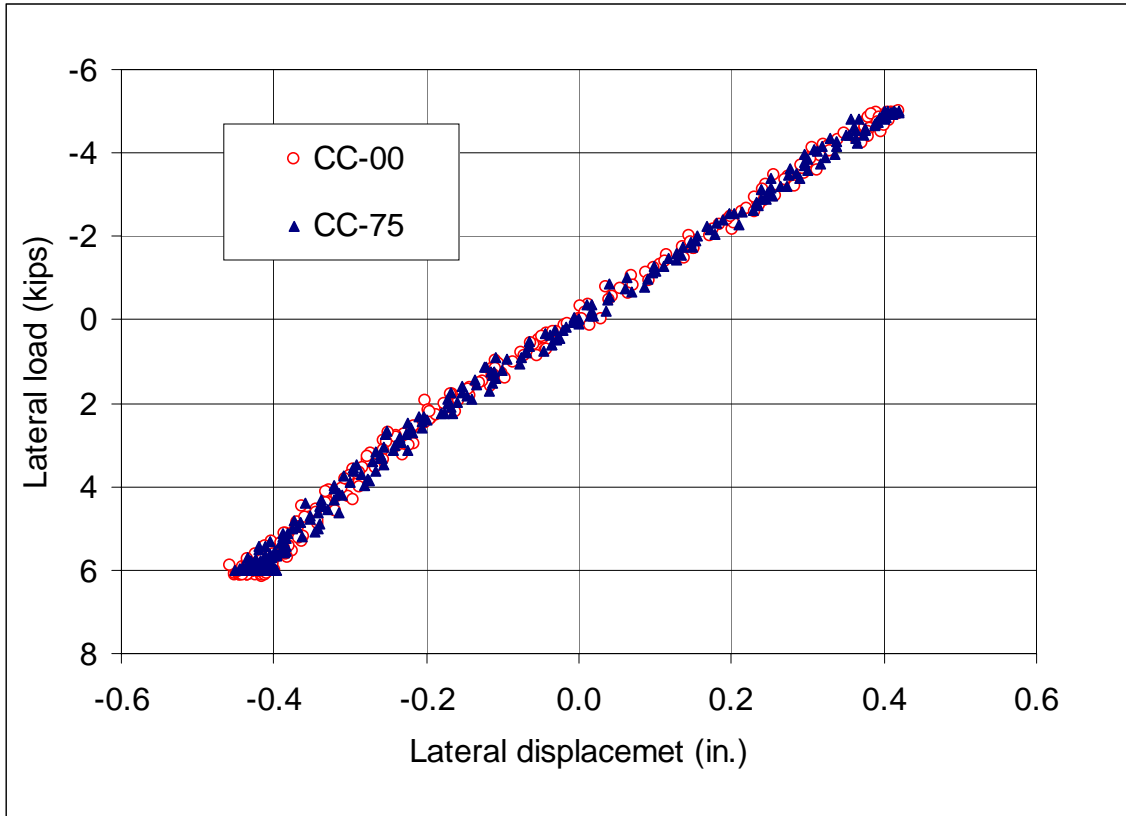


Figure 5.12. Lateral load vs. displacement relationship in HP-CC series

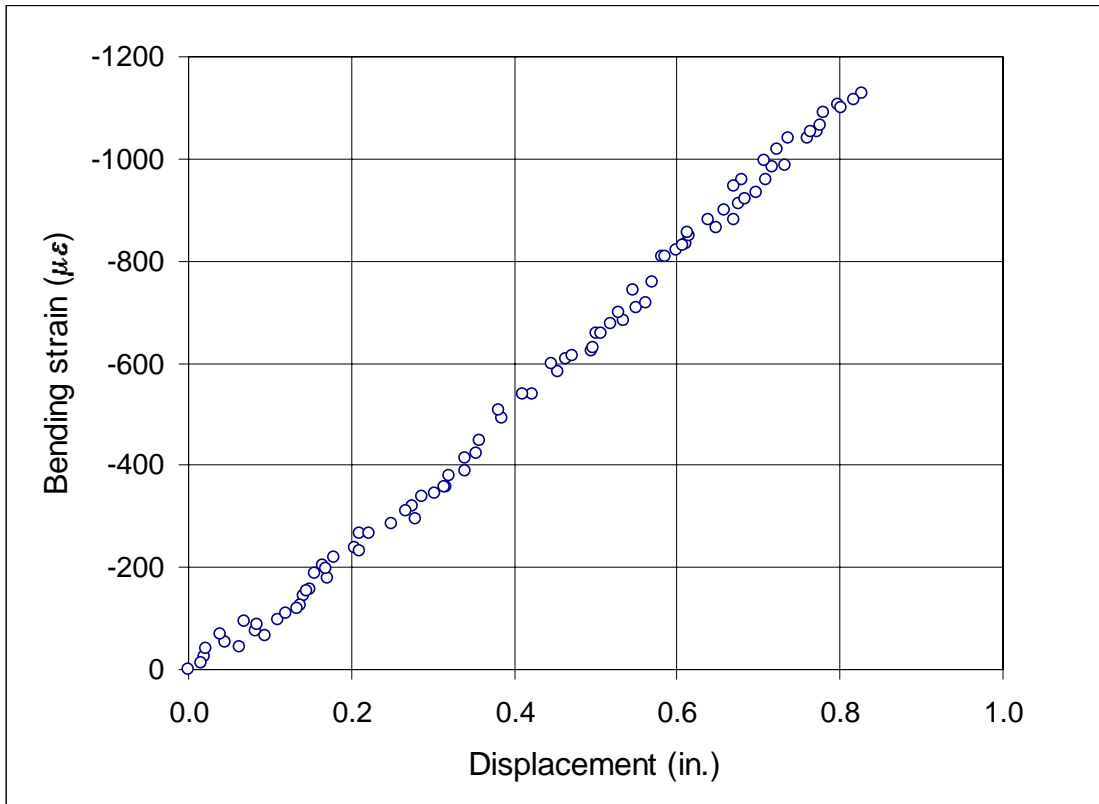


Figure 5.13. Lateral load vs. displacement relationship in HP-DD series

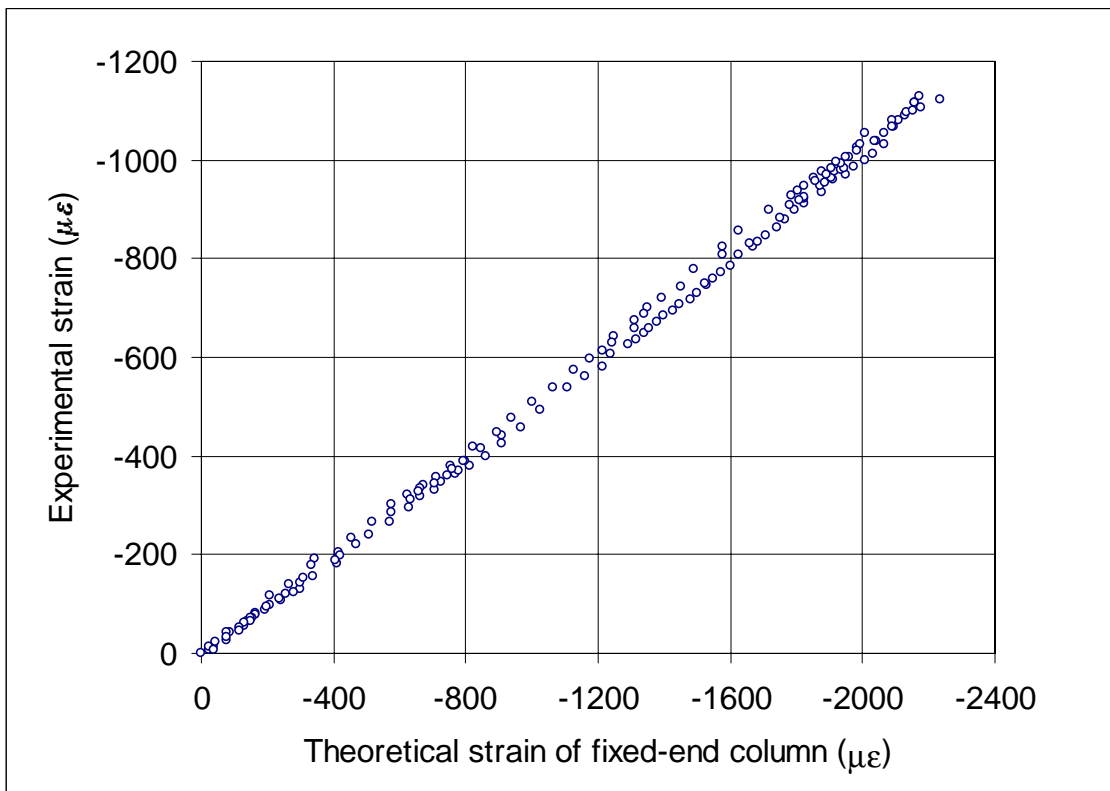


Figure 5.14. Experimental vs. theoretical strains of the H-pile test

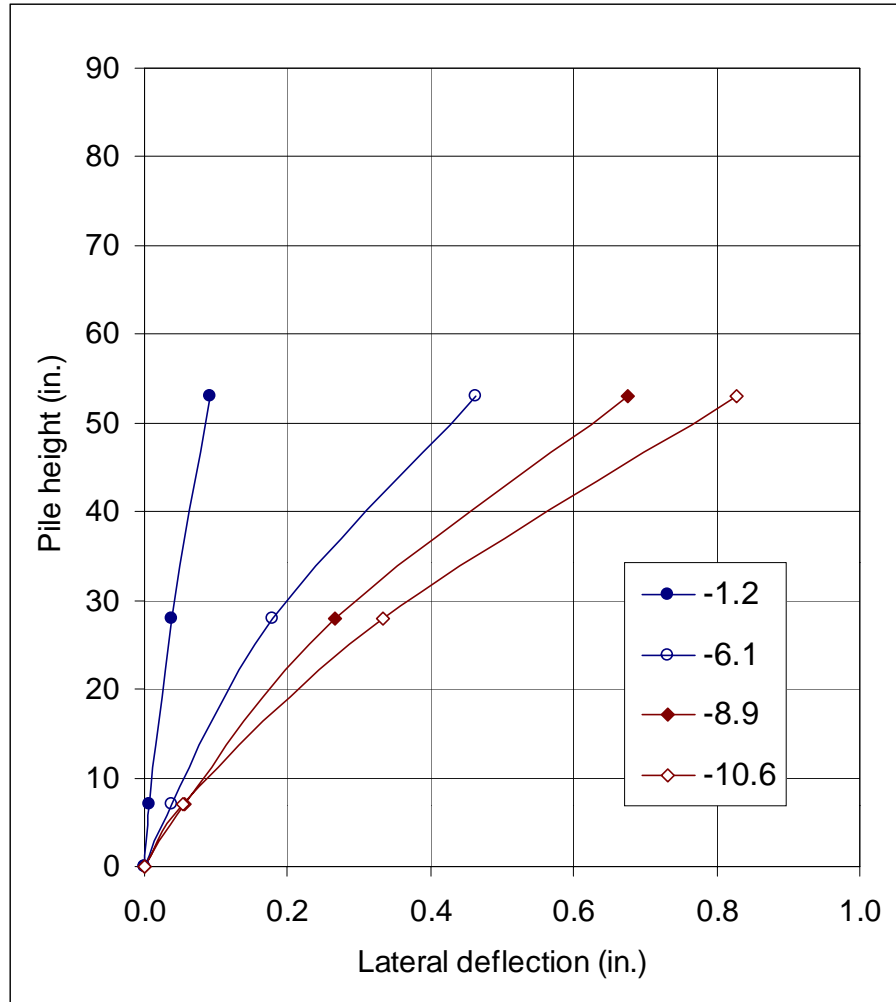


Figure 5.15. Displacements along the H-pile for selected lateral loads



Figure 5.16. Pictures of the damage observed in the pile cap during testing

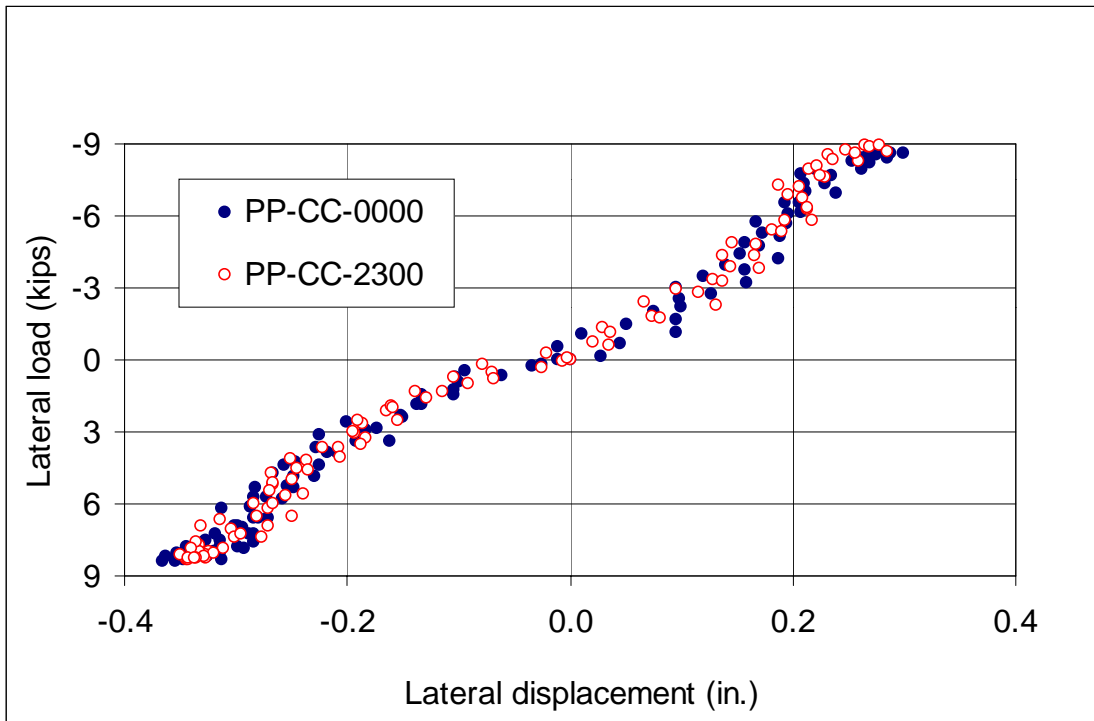


Figure 5.17. Lateral load vs. displacement relationship in pipe pile test

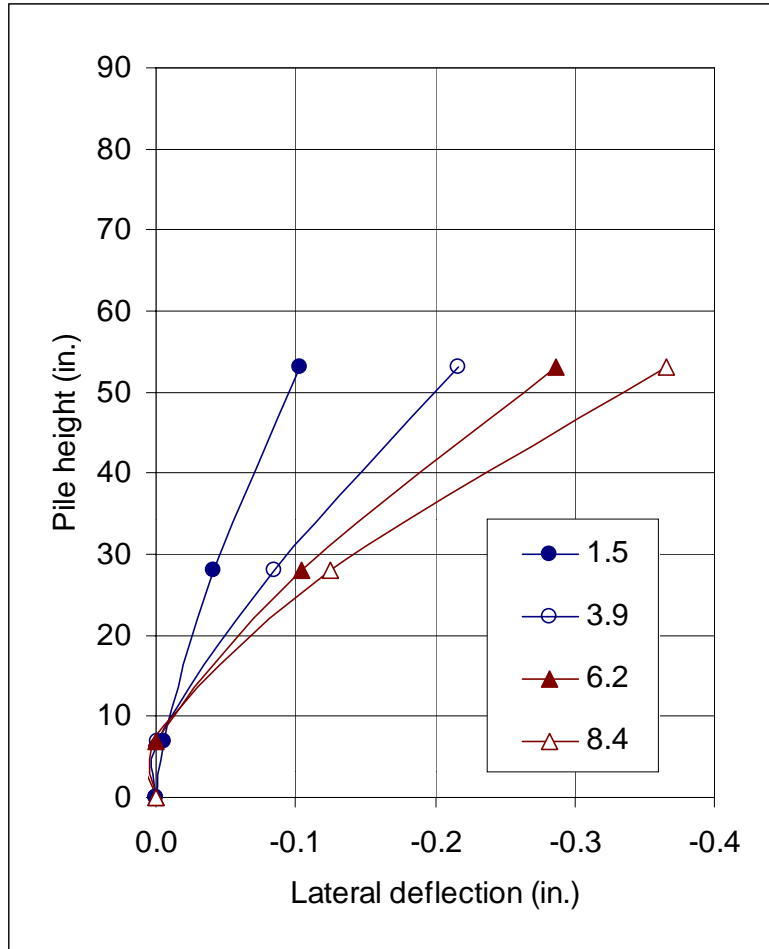


Figure 5.18. Displacements along the pipe pile for selected lateral loads in kips

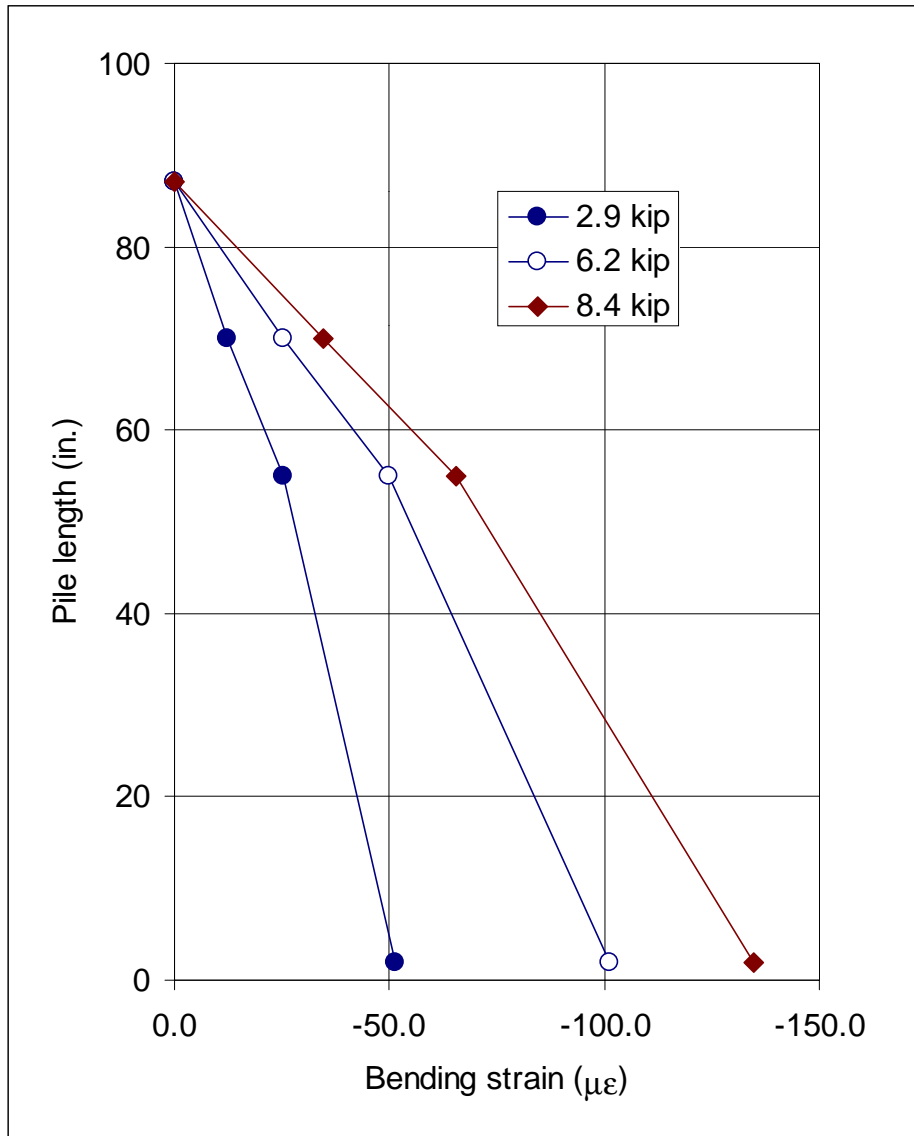


Figure 5.19. Bending strains along the pipe pile for selected lateral loads in kips

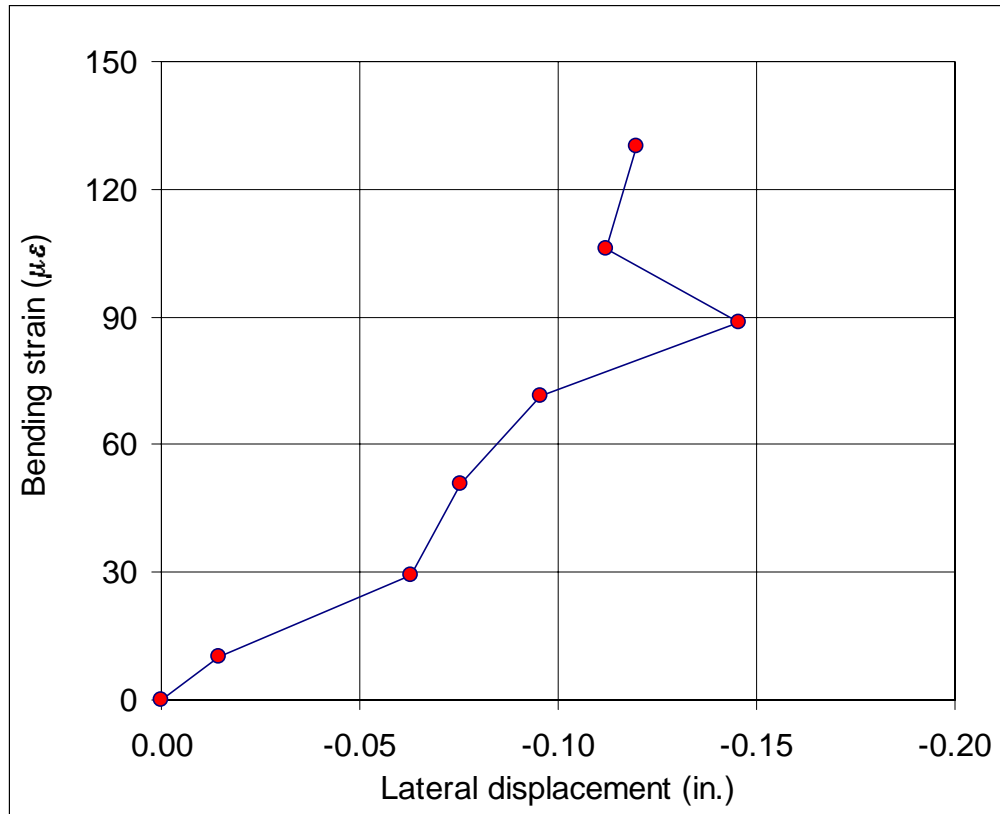


Figure 5.20. Failure of a strain gage because of tension cracks in the pile

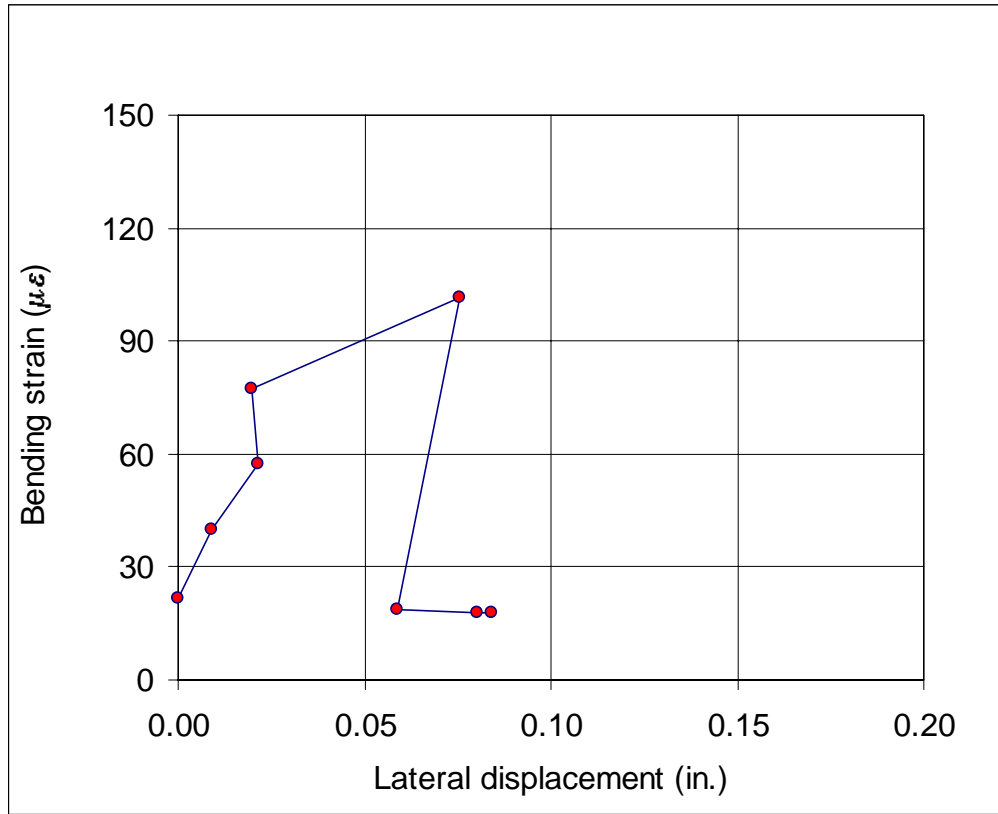


Figure 5.21. Drop in tension strain due to tension cracks as detected by a strain gage



Figure 5.22. Pictures of the tension cracks developed in the first load cycle

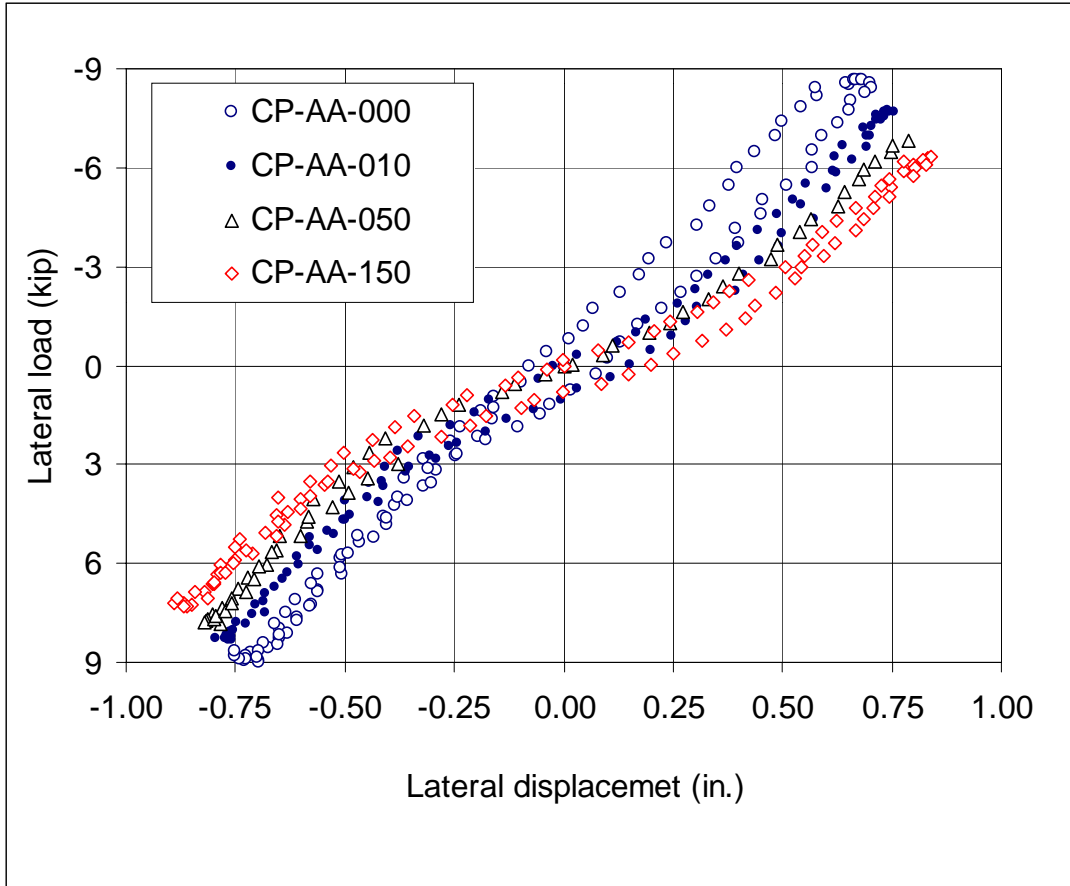


Figure 5.23. Lateral load vs. displacement relationship in CP-AA series



Figure 5.24. Progressively developed tension cracks in concrete pile

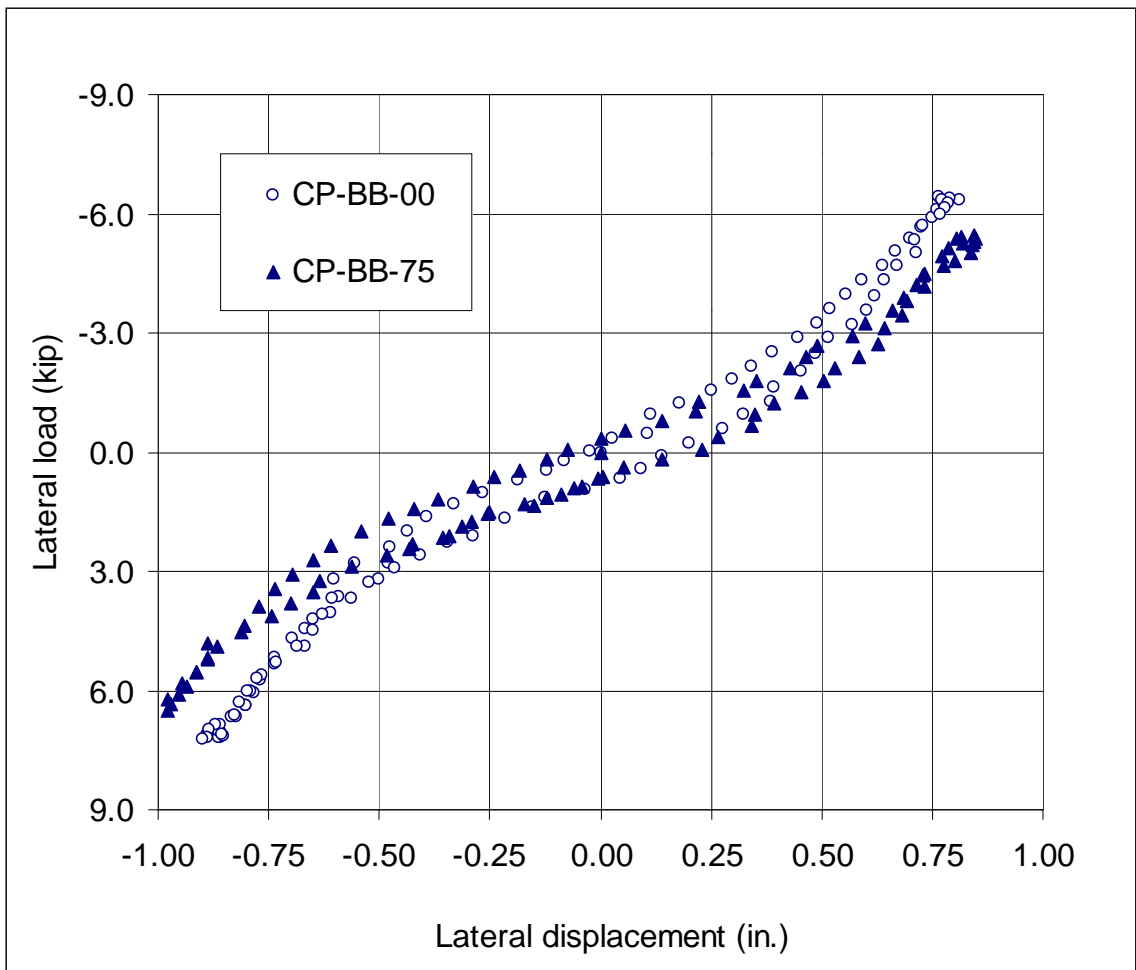


Figure 5.25. Lateral load vs. displacement relationship in CP-BB series

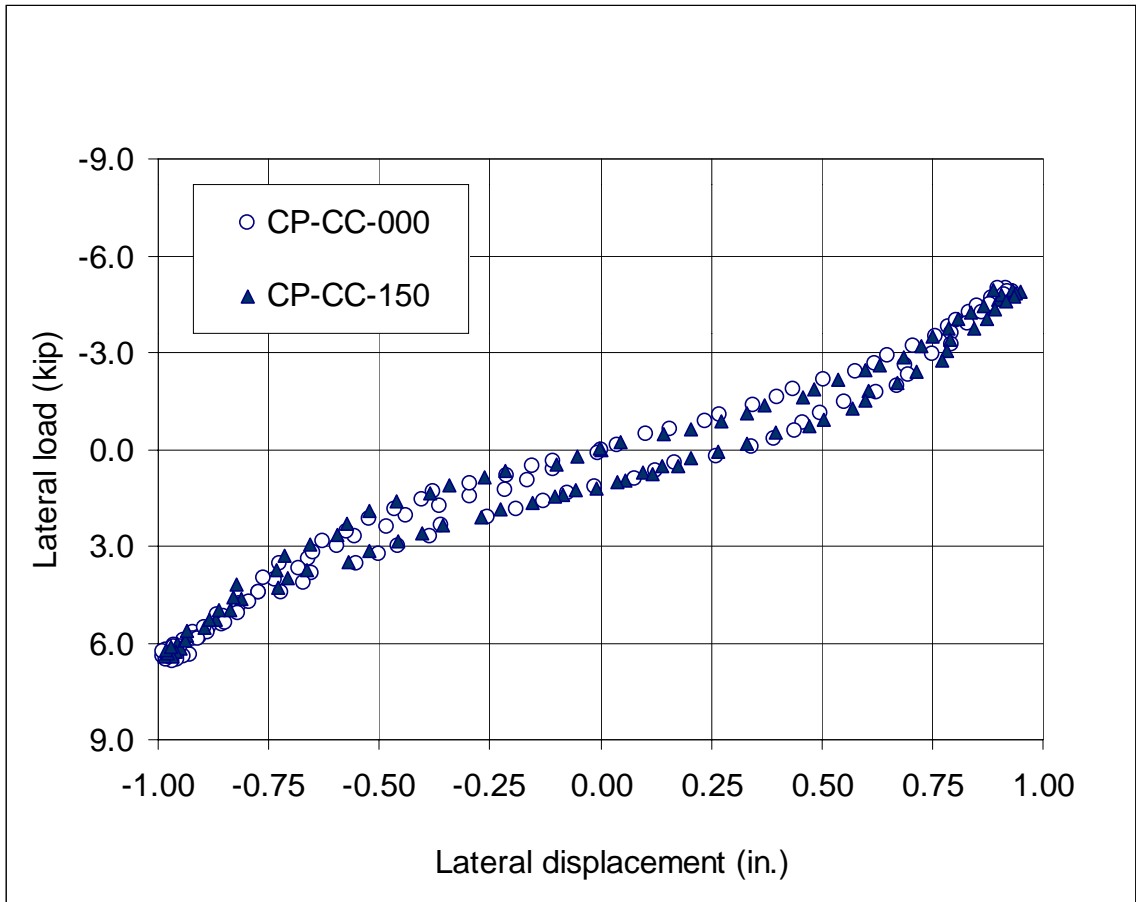


Figure 5.26. Lateral load vs. displacement relationship in CP-CC series